

Experimental Estimation of E-Field Distribution in a Vehicle under Multipath Propagation Environment Using a Reverberation Chamber

Katsushige Harima¹, Tetsuya Nakamura², Daich Akita², and Shinobu Ishigami³

¹ National Institute of Information and Communications Technology, Tokyo, Japan

² TOYO Corporation, Tokyo, Japan ³ Tohoku Gakuin University, Miyagi, Japan

Abstract - In this paper, we describe the maximum electric field (E-field) distribution in a vehicle under multipath propagation and single plane-wave exposure environments, as a basic study on radiated immunity testing for vehicles. The experimental estimation of the spatial field under these environments is performed using a reverberation chamber and an anechoic chamber. Experimental results obtained using a 1/5-scale vehicle model show that the E-field level in the vehicle under single plane-wave exposure is approximately 6 dB larger than that under a multipath propagation environment.

Index Terms — multipath propagation, reverberation chamber, Rayleigh distribution, field uniformity, electric field distribution in vehicle, radiated immunity testing.

1. Introduction

Today's vehicles are equipped with many electronic components such as electric control units for controlling the engine, transmission, windows, steering, and the like, and wireless radio systems. Electromagnetic compatibility (EMC) tests for these components and vehicle are carried out according to international standards [1][2]. Radiated immunity testing for vehicles is generally performed with a single plane-wave exposure using an anechoic chamber [2]. Meanwhile, reverberation chambers (RVC) are widely used for various EMC applications, such as radiated emissions, radiated immunity, shielding effectiveness, and antenna efficiency measurements [3], which exploit the characteristics of random fields in the chamber. The E-field strength in the RVC is Rayleigh-distributed [4], which closely resembles the fading distribution in wireless mobile communication. Thus, the use of a RVC is suitable for the EMC estimation of a vehicle under a real propagation environment.

In this paper, we estimate the E-field distribution in a 1/5-scale vehicle model at frequencies from 3 to 9 GHz under multipath propagation environment using a RVC, and compare it with a single plane-wave exposure case using an anechoic chamber.

2. Statistical Characteristics of E-Field Distribution

The RVC generally consists of a shielded enclosure with mechanical stirrers, as shown in Fig. 1. The E-field in the chamber varies by rotating the stirrers. The E-field is the vector sum of three rectangular components, each com-

ponent consisting of real and imaginary parts. As a large number of multipath waves arrive at a given location by moving the stirrers, each of these six components is normally distributed in accordance with the central limit theorem [4][5]. Under these conditions, the uniformity of the E-field distribution is expressed as a function of the number of independent stirrer positions, regardless of the operating frequency [6]. When the E-field is measured using a linearly polarized antenna, the received E-field strength is chi distributed with two degrees of freedom, which has the same characteristic as the Rayleigh distribution [4], which resembles the multipath propagation environment in wireless mobile communication.

3. Experiments and Results

The experimental setup is shown in Fig. 1. The RVC ($4 \times 3 \times 4.5 \text{ m}^3$) is equipped with four mechanical stirrers. A simplified 1/5-scale vehicle model ($0.3 \times 0.35 \times 1 \text{ m}^3$) was placed on a 3.5-cm-thick sheet of polystyrene foam in the chamber. The vehicle model consists of three parts, namely, engine, cabin, and trunk rooms. The vehicle body has apertures in the bottom of the engine room and in each side wall (windows) of the cabin, and the cabin and trunk rooms are connected spatially without a partition. The transmitting antenna was arranged so that it was not directed toward the vehicle model. The E-field in the vehicle model was measured using an isotropic E-field probe with an optical fiber link in 500 MHz steps from 3 to 9 GHz, which corresponds to a full-scale frequency from 0.6 to 1.8 GHz, while the stirrers were rotated continuously at different speeds (2, 4, 6, and 8 rpm). The three rectangular components, E_x , E_y , and E_z , were measured at 280 points sequentially over one

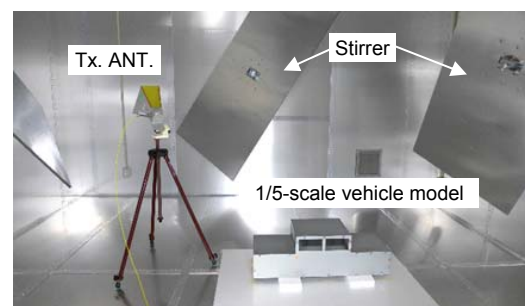


Fig. 1. Experimental set-up.

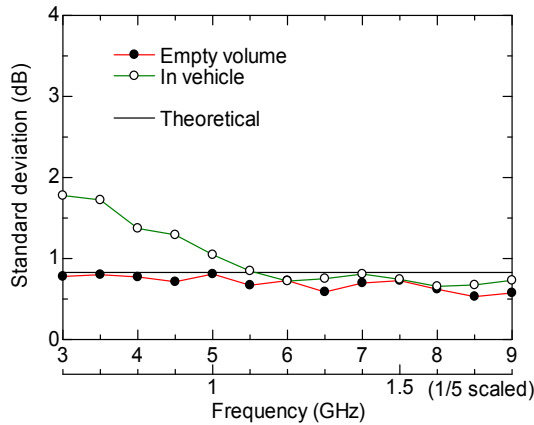


Fig. 2. Uniformity of the maximum E-field distribution in a vehicle model and without it measured at 51 probe locations using a RVC.

period of rotation (30 s) by the stirrers. The spatial distribution of the maximum field was evaluated from the maximum value ($E_{\max x}$, $E_{\max y}$, and $E_{\max z}$) of the obtained data at each of the 51 probe locations in the vehicle model.

Additionally, in order to compare with the single plane-wave environment, the maximum E-field distribution in the vehicle was evaluated using a semi-anechoic chamber (SAC). The transmitting antenna was arranged so as to illuminate directly the vehicle placed on the turntable at a distance of 2 m. The three rectangular components were measured sequentially during one rotation of the turntable. Next, the same measurements under these environments were performed without the vehicle model.

Figure 2 shows the uniformity of the maximum E-field distribution in the vehicle model using the RVC. The theoretical results obtained from the statistical characteristics described in the previous section are plotted in the same figure. In our numerical simulations, the spatial distribution of the maximum field is computed by repeatedly generating 280 items of random normally distributed data 5,000 times. The uniformity measured in the empty chamber, i.e., under the condition without a vehicle model, is in good agreement with the theoretical value. Thus, the field characteristic in the RVC can be assumed to be ideal at frequencies used in this estimation. The uniformity in the vehicle model above 5 GHz is approximately the same as that under the empty condition without the vehicle; however, it worsens gradually at lower frequencies owing to the effect of the cavity size of the vehicle.

Figure 3(a) shows the mean values of three rectangular components obtained in the engine, cabin, and trunk rooms of the vehicle model. The heat map of the maximum resultant field ($E_{\max res}$) is plotted in (b). These values are normalized by the values obtained under the condition without a vehicle. When using the RVC, i.e., under a multipath propagation environment, the average of $E_{\max x,y,z}$ in each room is the same as those condition without the vehicle, and the mean value of $E_{\max res}$ in all rooms is within approximately 1 dB. On the other hand, when using the

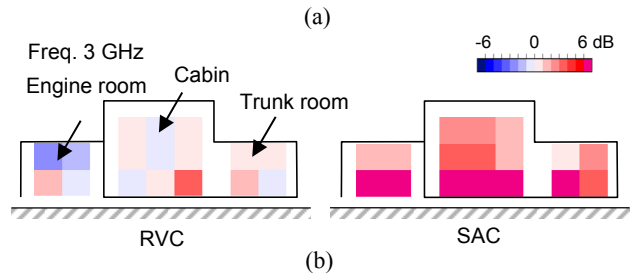
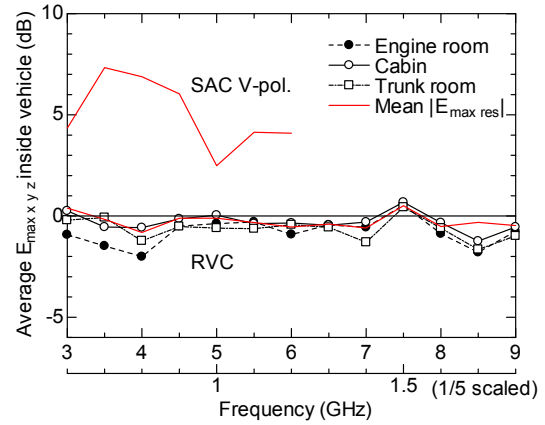


Fig. 3. (a) Average of the maximum E-field in each room of a vehicle model and (b) side cut view of vehicle for the maximum resultant field measured in a RVC and a SAC.

SAC, i.e., under a single incident wave environment, the maximum E-field in each room is greater than that under the multipath condition, and also the average of $E_{\max res}$ in all rooms is approximately 3 to 7 dB larger.

4. Conclusion

The spatial E-field distributions in a vehicle under a multipath propagation environment and single-plane wave exposure have been presented using a reverberation chamber and an anechoic chamber, respectively. Experimental results obtained using a simplified 1/5-scale vehicle model indicate the following: (1) under a multipath propagation environment, the uniformity of the maximum E-field distribution in the vehicle are approximately the same as those under the empty condition without the vehicle; (2) under a plane-wave exposure, the E-field strength in the vehicle is approximately 6 dB larger on average than that under a multipath propagation environment.

References

- [1] ISO 11452 series, Road vehicles – Components test methods –.
- [2] ISO 11451 series, Road vehicles – Vehicle test methods –.
- [3] IEC 61000-4-21, Reverberation chamber test methods, 2011.
- [4] G. Kostas, and B. Boverie, “Statistical model for a mode-stirred chamber,” *IEEE Trans. Electromagn. Compat.*, vol. 33, no. 4, pp. 366-370, Nov. 1991.
- [5] D.A. Hill, “Plane wave integral representation for fields in reverberation chambers,” *IEEE Trans. Electromagn. Compat.*, vol. 40, no. 3, pp. 209-217, Aug. 1998.
- [6] K. Harima, “Statistical characteristics of E-field distribution in a reverberation chamber,” *IEICE Trans. Commun.*, vol. E88-B, no. 8, pp. 3127-3232, July 2005.